

# Accuracy of apparent diffusion coefficient in differentiation of glioblastoma from metastasis

The Neuroradiology Journal  
0(0) 1–8  
© The Author(s) 2021  
Article reuse guidelines:  
sagepub.com/journals-permissions  
DOI: 10.1177/1971400920983678  
journals.sagepub.com/home/neu  
SAGE

Sanaz Beig Zali<sup>1</sup> , Farbod Alinezhad<sup>2</sup> , Mahnaz Ranjkesh<sup>3</sup>,  
Mohammad H Daghighi<sup>3</sup> and Masoud Poureisa<sup>3</sup>

## Abstract

**Background:** Brain metastasis and glioblastoma multiforme are two of the most common malignant brain neoplasms. There are many difficulties in distinguishing these diseases from each other.

**Purpose:** The purpose of this study was to determine whether the mean apparent diffusion coefficient and absolute standard deviation derived from apparent diffusion coefficient measurements can be used to differentiate glioblastoma multiforme from brain metastasis based on cellularity levels.

**Material and methods:** Magnetic resonance images of 34 patients with histologically verified brain tumors were evaluated retrospectively. Apparent diffusion coefficient and standard deviation values were measured in the enhancing tumor, peritumoral region, and contralateral healthy white matter. Then, to determine whether there was a statistical difference between brain metastasis and glioblastoma multiforme, we analyzed different variables between the two groups.

**Results:** Neither mean apparent diffusion coefficient values and ratios nor standard deviation values and ratios were significantly different between glioblastoma multiforme and brain metastasis. Receiver operating characteristic curve analysis of the logistic model with backward stepwise feature selection yielded an area under the curve of 0.77, a specificity of 84%, a sensitivity of 67%, a positive predictive value of 83.33%, and a negative predictive value of 78.26% for distinguishing between glioblastoma multiforme and brain metastasis. The absolute standard deviation and standard deviation ratios were significantly higher in the peritumoral edema compared to the tumor region in each case.

**Conclusion:** Apparent diffusion coefficient values and ratios, as well as standard deviation values and ratios in peritumoral edema, cannot be used to differentiate edema with infiltration of tumor cells from vasogenic edema. However, standard deviation values could successfully characterize areas of peritumoral edema from the tumoral region in each case.

## Keywords

Apparent diffusion coefficient, diffusion weighted imaging, glioblastoma multiforme, brain metastasis

## Introduction

Brain metastasis (BM) and glioblastoma multiforme (GBM) are two of the most commonly occurring central nervous system (CNS) neoplasms. GBM, as a primary brain tumor, accounts for 48.3% of malignant and 14.6% of all brain and CNS tumors. This tumor has a dismal prognosis with a five-year survival rate of 6.8%.<sup>1</sup> On the other hand, according to the most recent study on data collected by the Surveillance, Epidemiology, and End Results (SEER) program, BM is present in 2.0% of all cancer patients and 12.1% of patients with systemic metastatic disease at the time of primary cancer diagnosis.<sup>2,3</sup>

On conventional T1 and T2 weighted magnetic resonance imaging (MRI), both GBM and BM usually exhibit similar radiological appearances of a solitary, strongly enhancing brain tumor surrounded by T2-hyperintense edema, which leads to misdiagnosis in more than 40% of cases.<sup>4</sup> Nevertheless, due to

dissimilar treatment approaches, discrimination of these tumors in the preoperative period is of great importance. As a result, in most cases, a biopsy is performed to confirm the exact histopathology of the tumor.<sup>5–7</sup>

Although the anatomic MRI appearance of GBM and BM is similar, the microstructure of tumor capillaries and histopathology of peritumoral edema is markedly different between these tumors. GBM has a defective vessel formation that gives rise to vessels with variable diameters and permeability,

<sup>1</sup>Neuroscience Research Center, Tabriz University of Medical Sciences, Iran

<sup>2</sup>Student Research Committee, Tabriz University of Medical Sciences, Iran

<sup>3</sup>Department of Radiology, Tabriz University of Medical Sciences, Iran

### Corresponding author:

Farbod Alinezhad, Tabriz University of Medical Sciences, Golgasht Street, Postal code 5166/15731, Tabriz, Iran.  
Email: farbodaline@gmail.com

heterogeneous distribution, irregular basal lamina, and various degrees of blood-brain barrier (BBB) disruption.<sup>8</sup> The increase in capillary permeability and the breakdown of the BBB results in the retention of plasma fluid and protein in the extracellular space. This leads to a peritumoral T2 signal abnormality in MRI, which is termed as peritumoral edema. Moreover, GBM tends to grow in an infiltrative manner, typically invading the surrounding tissues microscopically for several centimeters beyond the area of the enhancing tumor. Therefore, peritumoral edema is better referred to as infiltrative edema in gliomas.

On the other hand, the capillaries in brain metastases resemble those from the site of the original systemic cancer, thus have no similarity to the normal brain capillaries and completely lack BBB components with prominent capillary fenestration, which results in greatly increased capillary permeability uniformly throughout the tumor vasculature, causing vasogenic edema. Metastatic tumors tend to grow in an expansile manner and typically displace the surrounding brain tissues rather than invading them. Therefore, the key to making a distinction between these two tumors appears to lie in detecting the differences within the peritumoral area.<sup>7,9</sup>

In recent years, researchers have suggested innovative ways for differentiating between brain tumors using advanced MRI modalities such as diffusion tensor imaging (DTI),<sup>10–12</sup> diffusion weighted imaging (DWI),<sup>4,6</sup> perfusion weighted imaging (PWI),<sup>13–16</sup> magnetic resonance spectroscopy,<sup>17</sup> or a combination of these methods.<sup>18–23</sup> Use of these methods, by evaluating tissue microstructure and tumor dynamics, can provide a more accurate evaluation of brain tumors.

This study focuses on DWI, a method that provides images based on the molecular motion of water. Within biological tissues, water movement is restricted by interactions with tissue compartments, cell membranes, and intracellular organelles. As a result, tissues with low cellularity or tissues containing ruptured cell membranes allow greater movement of water molecules and vice versa. The extent of water diffusion within biological tissues is measured with a parameter known as the apparent diffusion coefficient (ADC); ADC values are determined by diffusion weighting of the imaging sequence.<sup>24,25</sup>

BMs are known to be more cellular than gliomas due to the existence of compact sheets of tumor cells in their histological sections,<sup>26</sup> which leads to the hypothesis that ADC values derived from tumor regions of metastases would be lower than those of GBMs.

In GBM, peritumoral edema is filled with neoplastic cell infiltration causing more restricted water diffusion in comparison to the vasogenic edema of metastatic tumors. Therefore, we hypothesized that ADC values attributed to vasogenic edema of BMs would be higher than those from infiltrative edema of GBMs.

Moreover, we hypothesized that, as tumor infiltration declines from tumor core toward outer margins of peritumoral edema, there would be greater heterogeneity among ADC values derived from peritumoral regions of GBMs in comparison to BMs. Subsequently, the absolute standard deviation of ADC values attributed to GBMs would be greater.

We also hypothesized that increased water content in extracellular space in regions of T2 abnormality leads to increased water diffusivity and higher ADC of peritumoral edema compared to the tumor region, which can ultimately help precise delineation of tumor borders.

The purpose of this study is to examine the ADC values and their absolute standard deviations for both BM and GBM cases in order to look for any significant differences between them to determine whether the mean ADC and standard deviation (SD) derived from ADC measurements can be used to differentiate glioblastoma multiforme from BM based on cellularity levels in the enhancing tumor and in the peritumoral region. We also examine the differences in the ADC values between tumoral and peritumoral areas of each case as a potential method for tumor border delineation.

## Methods and materials

### Patients

All patients with probable diagnoses of GBM or BM referred to two MRI centers in the city from 2017–2019 were selected for follow-up.

All patients were contacted for informed consent agreement and follow-up from the imaging centers. The study was accepted by the ethics committee of Tabriz University.

Patients with a previous history of brain surgery before undergoing MRI, hemorrhagic brain tumors, inconclusive histopathology, absent peritumoral edema, and incomplete imaging sequences were excluded from the study.

The MRI examinations of 34 patients (14 women, 20 men; mean age  $56.1 \pm 12.8$  years; median age 57.5; age range 30–81 years) with histopathological diagnoses of GBM or BM were evaluated retrospectively.

The final diagnosis was based on histopathological findings. Of the 34 patients, GBM was diagnosed in 19 cases (11 men, eight women; mean age  $56.5 \pm 12$  years; median age 58; range 33–77 years), and BM was diagnosed in 15 cases (nine men, six women; mean age  $55.7 \pm 14.2$  years; median age 56; range 30–81 years). Metastatic brain tumors included carcinomas from lung ( $n=5$ ), thyroid ( $n=1$ ), renal cell carcinoma (RCC) ( $n=1$ ), squamous cell carcinoma (SCC) ( $n=1$ ), and unknown origin ( $n=7$ ).

### MRI and image processing

Examinations of all patients were performed using two identical 1.5-T MRI units (Magnetom Avanto,

Erlangen, Germany) in two MRI centers of the city. The conventional imaging protocol for solid brain tumors consisted of sagittal, coronal, and transverse T1-weighted spin-echo images before and after gadolinium-based contrast medium injection (repetition time (TR)=420 ms, time to echo (TE)=20 ms, field of view (FOV)=21.9 × 21.9, matrix size=256 × 220, slice thickness=5 mm, slice gap=2 mm), sagittal T2-weighted turbo spin echo scan (TR=4000 ms, TE=90 ms, FOV=21.9 × 21.9, matrix size=256 × 256, slice thickness=5 mm, slice gap=2 mm), and fluid-attenuated inversion recovery (FLAIR) scan (TR=4000 ms, TE=94 ms, inversion recovery time=1530 ms, FOV=22 × 22 cm<sup>2</sup>, matrix size=256 × 192, slice thickness=5 mm, slice gap=2 mm) Single-shot echo-planar diffusion-weighted images were acquired in the transverse plane with the acquisition of a diffusion trace and with the following parameters: TR=3200 ms, TE=94 ms, FOV=23.9 × 23.9, matrix size=192 × 192, slice thickness=5 mm, slice gap=2). Syngo.MR General Engine (Siemens, Erlangen, Germany), imaging acquisition and postprocessing software, was used to determine the ADC values.

Areas of pathological abnormalities were confirmed with the help of a radiologist. Round or oval-shaped regions of interest (ROIs) with an area of 0.25 cm<sup>2</sup> were carefully placed on three specified regions, avoiding contamination from different adjacent tissues with reference to conventional MRI. Inclusion of hemorrhagic, necrotic, and cystic areas in any ROIs were cautiously avoided. One ROI was positioned within the tumor borders corresponding to contrast agent enhancement region in T1 sequence, two ROIs within peritumoral edema corresponding to an area of hyperintense signal on T2-weighted images and no enhancement on post-contrast T1-weighted images, and one ROI in the contralateral healthy white matter (the region with normal signal intensity and no enhancement on T2 imaging).

The ADC values of the tumoral region (ADCT), healthy white matter (ADCN), the mean ADC value of peritumoral edema (ADCP), the absolute standard deviations of ADCT (SDT), the absolute standard deviation of ADCN (SDN), and the absolute standard deviation of ADCP (SDP) were recorded and selected for analysis. Figures 1 and 2 are, respectively, examples of GBM and BM cases that we studied and the methods we used for MRI evaluation and post-processing. The radiologists performing ROI placements were blinded to the tumor histopathology. The ROI placements were performed by two experienced neuroradiologists (MP and MHD), both with more than 20 years of experience in practicing and teaching neuroradiology and MRI assessment.

### Statistical analysis

ADC ratios and SD ratios were calculated by dividing tumoral or peritumoral ADC or SD values by their corresponding values of healthy white matter (ADCT ratio, ADCP ratio, SDT ratio, SDP ratio) and by dividing the ADC and absolute SD values in the tumor by the corresponding values of the peritumoral edema (ADCT/P ratio, SDT/P ratio). The ROI values were expressed in terms of 10<sup>-3</sup> mm<sup>2</sup>/s.

We used the R programming language to conduct our statistical analyses.<sup>27</sup> To compare the ADC and SD values and ratios in different areas (tumoral and peritumoral) for each case, we used paired *t*-tests. We have done one-sided *t*-tests to show if a value is significantly higher or lower in an area and two-sided *t*-tests to show if the values are not equal in these areas. No tests of normality were performed based on the central limit theorem and our sample size.<sup>28</sup> Analysis of variance (ANOVA) tests were used to compare the ADC and SD values and ratios between the metastasis and GBM cases. The threshold for significance was 0.05 for the abovementioned tests. To develop a predictive

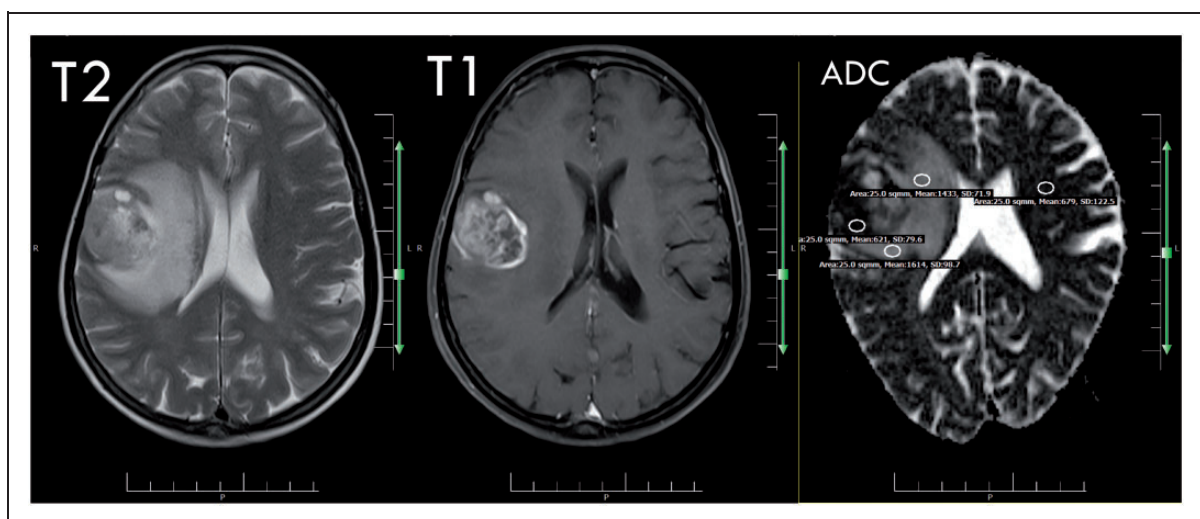


**Figure 1.** Glioblastoma multiforme (GBM) case evaluation and postprocessing. ADC: apparent diffusion coefficient; SD: standard deviation.

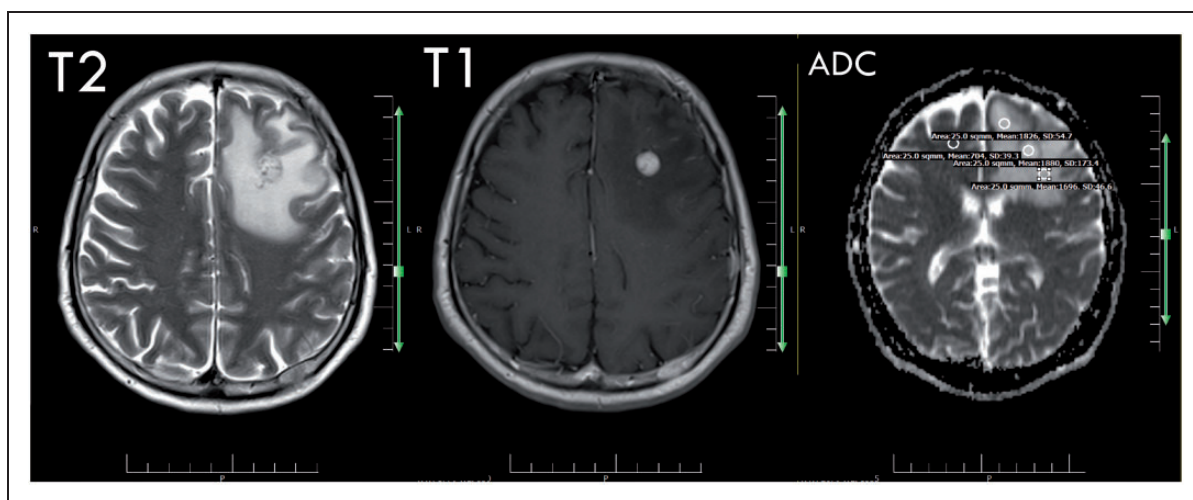


**Figure 2.** Brain metastasis case evaluation and postprocessing.

model based on our data, we have used the logistic regression method. The backward stepwise regression method was used for feature selection. Akaike information criterion was used as the criterion for feature subtraction. The results of the logistic regression model were used to draw receiver-operating characteristic (ROC) curves to calculate the sensitivity and specificity for different threshold levels in our model. We used the Youden's J statistic and closest.topleft values modified as proposed by Perkins and Schisterman to determine the optimal threshold (best trade-off between sensitivity and specificity).<sup>29</sup> The area under the curve (AUC) was used as a measure of the discriminatory performance of the model. We used the trapezoidal rule to calculate the AUC. We calculated 95% confidence intervals using 2000 stratified bootstrap replicates.

## Results

### *Differences of ADC and SD values between tumoral and peritumoral edema regions*

We have found no statistically significant difference between the values of ADCT-ADCP or ADCT ratio-ADCP ratio for each case ( $p$ -values respectively 0.1347 and 0.1397, paired  $t$ -test, two-sided). There was a significant difference between the values of SDT-SDP and SDT ratio-SDP ratio within each case ( $p$ -values, both less than 0.001, paired  $t$ -test, two-sided). Using one-sided  $t$ -tests for the former values (SDT-SDP and SDT ratio-SDP), we have found that the absolute SD and SD ratio values were significantly higher in the peritumoral edema compared to the tumoral region in each case (both  $p$ -values less than 0.001, paired  $t$ -test, one-sided). We have compared the same values within GBM and metastasis groups for each case, and the results were similar to what we have found for whole data.

**Table 1.** The  $p$ -values calculated using analysis of variance (ANOVA) for different variables between GBM and metastasis cases.

Variable	$p$ -value (ANOVA)
Age	0.87
ADCT	0.43
SDT	0.11
ADCP	0.36
SDP	0.91
ADCN	0.62
SDN	0.82
ADCT ratio	0.33
SDT ratio	0.14
ADCP ratio	0.29
SDP ratio	0.61
ADCT/P ratio	0.75
SDT/P ratio	0.1

ADCN: apparent diffusion coefficient of healthy white matter; ADCP: apparent diffusion coefficient of peritumoral edema; ADCT: apparent diffusion coefficient of the tumoral region; SDN: standard deviation of ADCN; SDP: standard deviation of ADCP; SDT: standard deviation of ADCT.

### *Differences of values between the metastasis and GBM groups*

We have found no significant differences between the metastasis and GBM groups for any of the variables in our study. Table 1 shows the  $p$ -values calculated using ANOVA for each of the variables between the two groups. Table 2 includes a summary of variables for all the cases and for the cases in each group. The results of analyses for possible differences in variables between metastases from different origins did not yield any significant results.

### *Using findings for predictive modeling*

Our backward stepwise logistic regression selected four variables, namely, ADCP, ADCN, ADCP ratio, and SDT/P ratio. The AUC of the ROC (95% confidence interval) of the model based on these variables was 0.77

**Table 2.** Summary of variables for all the cases and for the cases in each group.

Variable	All cases	GBM cases	Metastasis cases
ADCT	Mean (SD): 1433.5 (644.2)	Mean (SD): 1511.2 (714.4)	Mean (SD): 1335.2 (550.9)
SDT	Mean (SD): 145.2 (84.6)	Mean (SD): 124.7 (68.8)	Mean (SD): 171.2 (97.3)
ADCP	Mean (SD): 1726.6 (889.8)	Mean (SD): 1853.8 (1169.9)	Mean (SD): 1565.4 (237.6)
SDP	Mean (SD): 77 (24.6)	Mean (SD): 76.5 (27.5)	Mean (SD): 77.5 (21.2)
ADCN	Mean (SD): 755.8 (83.2)	Mean (SD): 749.3 (94)	Mean (SD): 764 (69.4)
SDN	Mean (SD): 77.6 (24.9)	Mean (SD): 78.5 (23.7)	Mean (SD): 76.6 (27.2)
ADCT ratio	Mean (SD): 1.9 (0.9)	Mean (SD): 2.1 (1)	Mean (SD): 1.7 (0.7)
SDT ratio	Mean (SD): 2.1 (1.5)	Mean (SD): 1.7 (1.2)	Mean (SD): 2.5 (1.7)
ADCP ratio	Mean (SD): 2.3 (1.2)	Mean (SD): 2.5 (1.5)	Mean (SD): 2.1 (0.3)
SDP ratio	Mean (SD): 1.1 (0.5)	Mean (SD): 1.1 (0.5)	Mean (SD): 1.2 (0.6)
ADCT/P ratio	Mean (SD): 0.9 (0.4)	Mean (SD): 0.9 (0.4)	Mean (SD): 0.9 (0.4)
SDT/P ratio	Mean (SD): 2 (1.3)	Mean (SD): 1.7 (1)	Mean (SD): 2.4 (1.5)

ADCN: apparent diffusion coefficient of healthy white matter; ADCP: apparent diffusion coefficient of peritumoral edema; ADCT: apparent diffusion coefficient of the tumoral region; SD: standard deviation; SDN: standard deviation of ADCN; SDP: standard deviation of ADCP; SDT: standard deviation of ADCT.

The SDT ratio is the absolute standard deviation of ADC value of tumor region divided by absolute standard deviation of its corresponding ADC value of healthy white matter, SDT/P ratio: absolute standard deviation of ADC value of tumor region divided by absolute standard deviation of its corresponding ADC value of peritumoral edema, full data = model using all 13 variables in Table 1.

(0.59–0.94). The ROC curve for the model is presented in Figure 3. Table 3 summarizes the sensitivity and specificities attained with three different thresholds (the threshold for best trade-off between sensitivity and specificity, the threshold where the sensitivity is 100%, and the threshold where the specificity is 100%) using the model.

## Discussion

Our study has shown that the ADC values ( $p = 0.43$ ) and ADC ratios ( $p = 0.32$ ) derived from tumor regions are not significantly different between the GBM and BM patients making DWI metrics obtained from tumor regions inaccurate for differentiating these tumors. This result is in line with the results of several other studies<sup>18,30–34</sup> investigating different sample sizes, ranging from 26–65 patients. Erver et al. in analyzing 59 patients with histologically verified high-grade gliomas and 23 patients with metastatic brain tumors reported significantly higher ADC values for GBM,<sup>35</sup> however, Krabbe et al. and Chiang et al. calculated comparatively significant higher ADC values for metastases.<sup>36,37</sup> Previous studies on DWI metrics of different brain tumors and abscesses have shown that other than cellularity, many factors can influence ADC values. Some factors, including reduced extracellular to intracellular space ratio, high nuclear to cytoplasm ratio, increased protein content, and micro-hemorrhages, are correlated with reduced ADCs, while others such as necrotic and cystic changes are known to increase it.<sup>38–43</sup> The heterogeneity in the findings, as mentioned above, maybe due to the presence of these factors.

We found no statistically significant differences between the values of ADCT-ADCP or ADCT ratio-ADCP ratio for each of GBM or BM cases; however, comparing SDT and SDT ratio with SDP and SDP

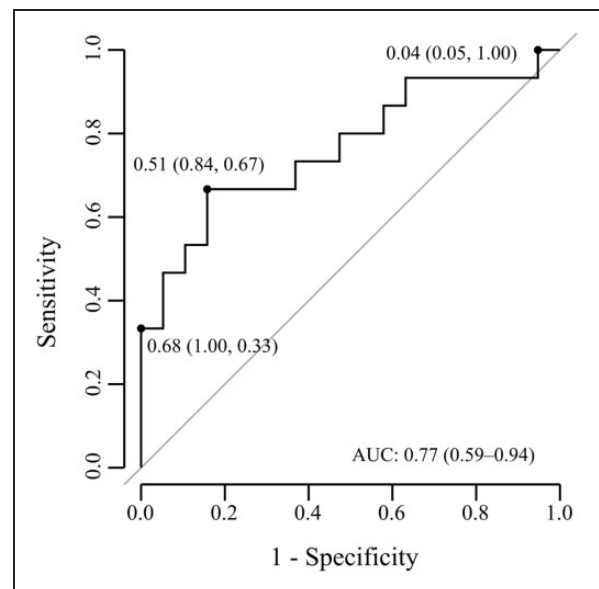


**Figure 3.** The receiver-operating characteristic (ROC) curve for the logistic model with the area under curve (AUC) (95% confidence interval) as well as the sensitivity and specificity values for different thresholds (the threshold for best trade-off between sensitivity and specificity, the threshold where the sensitivity is 100%, and the threshold where the specificity is 100%).

ratio, respectively, within each case resulted in a highly significant difference, with higher measures attributed to peritumoral edema in comparison to tumor region for both types of tumors. Statistically significant higher absolute SDs for ADC values of peritumoral edema regions compared to those of tumor regions, in our opinion, represents the difference between heterogeneity of ADC values attributed to these areas (probably due to the heterogeneity in the peritumoral edema compared to the tumor tissue) and can help in differentiation of tumor borders from

**Table 3.** Receiver-operating characteristic (ROC) curve analysis for different thresholds (the threshold for best trade-off between sensitivity and specificity, the threshold where the sensitivity is 100%, and the threshold where the specificity is 100%).

	Threshold	% (95% CI)
Best trade-off: sensitivity	0.51	66.67% (40.00–100.00)
Best trade-off: specificity	0.51	89.47% (47.37–100.00)
Best trade-off: PPV	0.51	83.33% (57.69–100.00)
Best trade-off: NPV	0.51	78.26% (65.52–100.00)
Sensitivity 100%: specificity	0.04	5.26% (5.26–15.79)
Sensitivity 100%: PPV	0.04	45.45% (45.45–48.39)
Sensitivity 100%: NPV	0.04	100.00%
Specificity 100%: sensitivity	0.68	33.33% (13.33–60.00)
Specificity 100%: PPV	0.68	100.00%
Specificity 100%: NPV	0.68	65.52% (59.38–76.00)

CI: confidence interval; NPV: negative predictive value; PPV: positive predictive value.

peritumoral edema in further evaluation of intracranial tumors.

Oh et al.<sup>26</sup> observed higher ADC values in the regions of peritumoral edema compared to regions of the contrast-enhancing tumor for both metastasis and GBM. Conversely, Sinha et al. showed higher ADC values in the enhancing tumor regions for high-grade gliomas,<sup>44</sup> while others report similar ADC values between those regions.<sup>32,45</sup>

The results of our study did not show any significant difference between peritumoral ADC values and ratios of GBM and BM. Likewise, corresponding SD values and ratios had no significant differences. To our knowledge, there are many discrepancies between authors in regards to the usefulness of ADC measurements for differentiating areas of vasogenic edema from infiltrative edema, hence BM from GBM. We have found many studies both in agreement<sup>32,35,46,47</sup> and in disagreement<sup>33,36,37,47,48</sup> with our results. Low sample sizes, differences in group-size, subjective bias caused by manually placing ROIs, different image acquisition specifications such as different B values, and differences in the primary site of tumors studied may be some of the contributing factors to varying results across studies. Studies show that metastases from different primary tumor sites cause different degrees of peritumoral edema, which may also have different characteristics in ADC values. As an example, metastases from adenocarcinomas and squamous cell carcinomas are known to cause higher degrees of edema in comparison to small cell lung cancers.<sup>49,50</sup> Yet, divergence among pieces of evidence may suggest that the practicality of ADC measurements for characterization of peritumoral signal changes is uncertain.

The limitations of our study include, first, that the case selection was performed with a retrospective approach. Second, as in all other ROI-based studies, inherent subjectivity in the manual placement of the ROIs might have influenced the accuracy of the ADC measurements. We used the same sized ROIs and

avoided including hemorrhagic or necrotic regions to decrease the inaccuracies in this regard. Third, our study, as well as previous studies, lacks precise stereotactic biopsies to directly correlate ADC measurements in ROIs with tumor histopathologies in exactly similar areas. We used, however, pathological results from leading pathologists in the city who had a good record of accomplishment in tissue diagnosis.

In conclusion, SD values could successfully characterize areas of peritumoral edema from the tumor region in each case and could be used for further delineation of tumor borders. Neither mean ADC values and ratios nor mean SD values and ratios in peritumoral brain regions were useful in determining the presence of peritumoral neoplastic cell infiltration. In addition, our results showed that mean ADC values of the tumor as not a reliable diagnostic tool for differentiation of GBM from BMs.

### Conflict of interest


The authors declared no potential conflicts of interest with respect to the research, authorship, and/or publication of this article.

### Funding

This research received no specific grant from any funding agency in the public, commercial, or not-for-profit sectors.

### ORCID iDs

Sanaz Beig Zali  <https://orcid.org/0000-0002-5284-0728>

Farbod Alinezhad  <https://orcid.org/0000-0003-1050-8310>

### References

- Ostrom QT, Cioffi G, Gittleman H, et al. CBTRUS statistical report: primary brain and other central nervous system tumors diagnosed in the United States in 2012–2016. *Neuro-Oncology* 2019; 21: V1–V100.
- Ostrom QT, Wright CH and Barnholtz-Sloan JS. Brain metastases: Epidemiology. In: Schiff D and Van den Bent MJ (eds.) *Handbook of clinical neurology*, Vol. 149. Elsevier, 2018, pp.27–42. Available at: <https://www.sciencedirect.com/science/article/pii/B9780128111611000025>
- Bucholtz JD. *Central nervous system metastases*. In: Ramakrishna R, Magge RS, Baaj AA and Knisely JPS (eds.) Cham: Springer International Publishing, 2020; pp.53–67.
- Lemercier P, Maya SP, Patrie JT, et al. Gradient of apparent diffusion coefficient values in peritumoral edema helps in differentiation of glioblastoma from solitary metastatic lesions. *Am J Roentgenol* 2014; 203: 163–169.
- Darefsky AS, King JT, Dubrow R. Adult glioblastoma multiforme survival in the temozolomide era: A population-based analysis of surveillance, epidemiology, and end results registries. *Cancer* 2012; 118: 2163–2172.
- Bulakbasi N, Guvenc I, Onguru O, et al. The added value of the apparent diffusion coefficient calculation to magnetic resonance imaging in the differentiation and grading of malignant brain tumors. *J Comput Assist Tomogr* 2004; 28: 735–746.

7. Cha S, Lupo JM, Chen MH, et al. Differentiation of glioblastoma multiforme and single brain metastasis by peak height and percentage of signal intensity recovery derived from dynamic susceptibility-weighted contrast-enhanced perfusion MR imaging. *Am J Neuroradiol* 2007; 28: 1078–1084.
8. Dubois LG, Campanati L, Righy C, et al. Gliomas and the vascular fragility of the blood brain barrier. *Front Cell Neurosci* 2014; 8: 1–13.
9. Lee EJ, Ahn KJ, Lee EK, et al. Potential role of advanced MRI techniques for the peritumoural region in differentiating glioblastoma multiforme and solitary metastatic lesions. *Clinical Radiology* 2013; 68: e689–e697.
10. Cha S, Knopp EA, Johnson G, et al. Intracranial mass lesions: Dynamic contrast-enhanced susceptibility-weighted echo-planar perfusion MR imaging. *Radiology* 2002; 223: 11–29.
11. Zhang P and Liu B. Differentiation among glioblastomas, primary cerebral lymphomas, and solitary brain metastases using diffusion-weighted imaging and diffusion tensor imaging: A PRISMA-compliant meta-analysis. *ACS Chem Neurosci* 2020; 11: 477–483.
12. Toh CH, Wei KC, Ng SH, et al. Differentiation of brain abscesses from necrotic glioblastomas and cystic metastatic brain tumors with diffusion tensor imaging. *Am J Neuroradiol* 2011; 32: 1646–1651.
13. Lee MD, Baird GL, Bell LC, et al. Utility of percentage signal recovery and baseline signal in DSC-MRI optimized for relative CBV measurement for differentiating glioblastoma, lymphoma, metastasis, and meningioma. *Am J Neuroradiol* 2019; 40: 1445–1450.
14. Lehmann P, Saliou G, De Marco G, et al. Cerebral peritumoral oedema study: Does a single dynamic MR sequence assessing perfusion and permeability can help to differentiate glioblastoma from metastasis? *Eur J Radiol* 2012; 81: 522–527.
15. Mangla R, Kolar B, Zhu T, et al. Percentage signal recovery derived from MR dynamic susceptibility contrast imaging is useful to differentiate common enhancing malignant lesions of the brain. *Am J Neuroradiol* 2011; 32: 1004–1010.
16. Sparacia G, Gadde JA, Iaia A, et al. Usefulness of quantitative peritumoural perfusion and proton spectroscopic magnetic resonance imaging evaluation in differentiating brain gliomas from solitary brain metastases. *Neuroradiol J* 2016; 29: 160–167.
17. Opstad KS, Murphy MM, Wilkins PR, et al. Differentiation of metastases from high-grade gliomas using short echo time 1H spectroscopy. *J Magn Reson Imaging* 2004; 20: 187–192.
18. Calli C, Kitis O, Yuntun N, et al. Perfusion and diffusion MR imaging in enhancing malignant cerebral tumors. *Eur J Radiol* 2006; 58: 394–403.
19. Rizzo L, Crasto SG, Moruno PG, et al. Role of diffusion- and perfusion-weighted MR imaging for brain tumour characterisation. *Radiol Med* 2009; 114: 645–659.
20. Abdel Razeq AAK, Talaat M, El-Serougy L, et al. Differentiating glioblastomas from solitary brain metastases using arterial spin labeling perfusion- and diffusion tensor imaging-derived metrics. *World Neurosurg* 2019; 127: e593–e598.
21. Zhao J, Yang ZY, Luo BN, et al. Quantitative evaluation of diffusion and dynamic contrast-enhanced MR in tumor parenchyma and peritumoral area for distinction of brain tumors. *PLoS One* 2015; 10: 1–15.
22. Chen R, Wang S, Poptani H, et al. A Bayesian diagnostic system to differentiate glioblastomas from solitary brain metastases. *Neuroradiol J* 2013; 26: 175–183.
23. Al-Okaili RN, Krejza J, Woo JH, et al. Intraaxial brain masses: MR imaging-based diagnostic strategy – initial experience. *Radiology* 2007; 243: 539–550.
24. Dubey A, Kataria R and Sinha V. Role of diffusion tensor imaging in brain tumor surgery. *Asian J Neurosurg* 2018; 13: 302.
25. Al-Okaili RN, Krejza J, Wang S, et al. Advanced MR imaging techniques in the diagnosis of intraaxial brain tumors in adults. *Radiographics* 2006; 26: S173–S189.
26. Oh J, Cha S, Aiken AH, et al. Quantitative apparent diffusion coefficients and T2 relaxation times in characterizing contrast enhancing brain tumors and regions of peritumoral edema. *J Magn Reson Imaging* 2005; 21: 701–708.
27. R Foundation for Statistical Computing. 3.5.1. *RDCCT. A language and environment for statistical computing*, <https://www.R-project.org> (2018).
28. Kwak SG and Kim JH. Central limit theorem: The cornerstone of modern statistics. *Korean J Anesthesiol* 2017; 70: 144–156.
29. Perkins NJ and Schisterman EF. The inconsistency of ‘optimal’ cutpoints obtained using two criteria based on the receiver operating characteristic curve. *Am J Epidemiol* 2006; 163: 670–675.
30. Yamasaki F, Kurisu K, Satoh K, et al. Apparent diffusion coefficient of human brain tumors at MR imaging. *Radiology* 2005; 235: 985–991.
31. Stadnik TW, Shabana WM, Luypaert R, et al. Diffusion-weighted MR imaging of intracerebral masses: Comparison with conventional MR imaging and histologic findings. *Am J Neuroradiol* 2001; 22: 969–976.
32. Kono K, Inoue Y, Nakayama K, et al. The role of diffusion-weighted imaging in patients with brain tumors. *Am J Neuroradiol* 2001; 22: 1081–1088.
33. Lee EJ, TerBrugge K, Mikulis D, et al. Diagnostic value of peritumoral minimum apparent diffusion coefficient for differentiation of glioblastoma multiforme from solitary metastatic lesions. *Am J Roentgenol* 2011; 196: 71–76.
34. Neska-Matuszewska M, Bladowska J, Sasiadek M, et al. Differentiation of glioblastoma multiforme, metastases and primary central nervous system lymphomas using multiparametric perfusion and diffusion MR imaging of a tumor core and a peritumoral zone – searching for a practical approach. *PLoS One*; 13(1): e0191341.
35. Server A, Kulle B, Mhlen J, et al. Quantitative apparent diffusion coefficients in the characterization of brain tumors and associated peritumoral edema. *Acta Radiol* 2009; 50: 682–689.
36. Krabbe K, Gideon P, Wagn P, et al. MR diffusion imaging of human intracranial tumours. *Neuroradiology* 1997; 39: 483–489.
37. Chiang IC, Kuo YT, Lu CY, et al. Distinction between high-grade gliomas and solitary metastases using peritumoral 3-T magnetic resonance spectroscopy, diffusion, and perfusion imagings. *Neuroradiology* 2004; 46: 619–627.
38. Chang SC, Lai PH, Chen WL, et al. Diffusion-weighted MRI features of brain abscess and cystic or necrotic

- brain tumors: Comparison with conventional MRI. *Clin Imaging* 2002; 26: 227–236.
39. Humphries PD, Sebire NJ, Siegel MJ, et al. Tumors in pediatric patients at diffusion-weighted MR imaging: Apparent diffusion coefficient and tumor cellularity. *Radiology* 2007; 245: 848–854.
  40. Leite C da C, Leite C da C, Castillo M (eds). *Diffusion weighted and diffusion tensor imaging: A clinical guide*. Stuttgart: Georg Thieme Verlag, 2016.
  41. Higano S, Yun X, Kumabe T, et al. Malignant astrocytic tumors. 2006; 241: 839–846.
  42. Doty FD, Entzminger G, Kulkarni J, et al. Radio frequency coil technology for small-animal MRI. *NMR Biomed* 2007; 20: 304–325.
  43. Rose S, Fay M, Thomas P, et al. Correlation of MRI-derived apparent diffusion coefficients in newly diagnosed gliomas with [18F]-Fluoro-L-Dopa PET: What are we really measuring with minimum ADC? *Am J Neuroradiol* 2013; 34: 758–764.
  44. Sinha S, Bastin ME, Whittle IR, et al. Diffusion tensor MR imaging of high-grade cerebral gliomas. *Am J Neuroradiol* 2002; 23: 520–527.
  45. Castillo M, Smith JK, Kwock L, et al. Apparent diffusion coefficients in the evaluation of high-grade cerebral gliomas. *Am J Neuroradiol* 2001; 22: 60–64.
  46. Tropine A, Vucurevic G, Delani P, et al. Contribution of diffusion tensor imaging to delineation of gliomas and glioblastomas. *J Magn Reson Imaging* 2004; 20: 905–912.
  47. Lu S, Ahn D, Johnson G, et al. Diffusion-tensor MR imaging of intracranial neoplasia and associated peritumoral edema: Introduction of the tumor infiltration index. *Radiology* 2004; 232: 221–228.
  48. Van Westen D, Lätt J, Englund E, et al. Tumor extension in high-grade gliomas assessed with diffusion magnetic resonance imaging: Values and lesion-to-brain ratios of apparent diffusion coefficient and fractional anisotropy. *Acta Radiol* 2006; 47: 311–319.
  49. Baris MM, Celik AO, Gezer NS, et al. Role of mass effect, tumor volume and peritumoral edema volume in the differential diagnosis of primary brain tumor and metastasis. *Clin Neurol Neurosurg* 2016; 148: 67–71.
  50. Fábrián K, Gyulai M, Furák J, et al. Significance of primary tumor location and histology for brain metastasis development and peritumoral brain edema in lung cancer. *Oncology* 2016; 91: 237–242.